Available online at www.sciencedirect.com
SCIENCE DIRECT®
Diamond and Related Materials 13 (2004) 1287–1291
DIAMOND AND RELATED MATERIALS
www.elsevier.com/locate/diamond

Experimental studies of the formation process and morphologies of carbon nanotubes with bamboo mode structures

Y.Y. Wang*, G.Y. Tang, F.A.M. Koeck, Billyde Brown, J.M. Garguilo, R.J. Nemanich

Department of Physics and Department of Material Science and Engineering, North Carolina State University, Raleigh, NC 27695-8202, USA

Abstract

Carbon nanotubes (CNT) were synthesized by microwave plasma chemical vapor deposition, and the formation process and morphologies of bamboo mode structures were systematically analyzed. Thin films of Fe on Si substrates were used as the catalyst, and the CNT films were characterized with electron microscopy, Raman spectroscopy, and Auger electron spectroscopy. For growth up to 15 min, the films grow with vertically aligned CNT with evidence of amorphous carbon at the top surface. For longer growth times the films exhibit a layer of amorphous carbon and a CNT mat on top of the aligned carbon nanotube 'forest.' Transmission electron microscopy measurements displayed multiwalled CNT with bamboo structure and encapsulated tips some of which contained catalyst particles. Two kinds of bamboo mode structures were observed: cone shaped, and cylindrical. The results indicate that the CNT growth is predominantly of the base growth mode, and the formation of the compartments was attributed to the difference in the bulk and surface diffusion of carbon species at the catalyst.

Keywords: Multiwalled carbon nanotubes; Bamboo mode; Formation process; Morphologies

1. Introduction

With their unique structural, chemical, electronic, and mechanical properties [1], carbon nanotubes exhibit potential as field emitters [2], nanometer-sized transistors [3], and sensors [4]. Recently, Zettl et al. fabricated the world's smallest motor based on carbon nanotubes [5], which furthers the application to nanoelectromechanical systems (NEMS).

Carbon nanotubes (CNT) can be grown in large quantities by chemical vapor deposition (CVD). Transition metals such as iron, nickel, and cobalt are commonly used to catalyze the growth [1]. The growth mechanisms have been studied theoretically and experimentally [6–9], and two modes have been observed: base growth and tip growth. The tip growth mode is evidenced by metal particles at the tips of carbon nanotubes, while the metal particles remain attached to the substrate for the base growth mode [10].

The bamboo structure observed in multiwalled CNT is characterized by segmented compartments, which appear similar to a bamboo. Several studies have presented explanations for the origin of these periodic structures [7,11–13]. It was suggested that the bamboo structures might be due to effects related to the catalyst particle shape, the bulk diffusion of carbon in the catalyst, or the slow movement of the catalyst compared to the growth rate of the CNT. In this study, we experimentally study the growth mode and bamboo structure of multiwalled carbon nanotubes. We have interpreted the results as indicating that the base growth mode predominates in our CNT growth, and that the bamboo structure is due to effects related to the diffusion of carbon in the catalyst.

2. Experimental details

In this study, films of vertically aligned carbon nanotubes were grown using a microwave plasma enhanced CVD system (MPCVD). The alignment of CNT in MPCVD has been attributed to the electric field at the edge of the plasma [14]. We note that the same growth chamber can also be used to grow diamond films [15]. The catalyst used was an 80 nm iron film, which was deposited on silicon wafers by DC magnetron sputtering. The iron-coated silicon was loaded into the MPCVD chamber, the chamber was pumped to 10^{-3} Torr, a

*Corresponding author. Tel.: +1-919-515-2474; fax: +1-919-515-7331.
E-mail address: ywang10@unity.ncsu.edu (Y.Y. Wang).

0925-9635/04/$ - see front matter © 2004 Elsevier B.V. All rights reserved.
doi:10.1016/j.diamond.2004.01.009

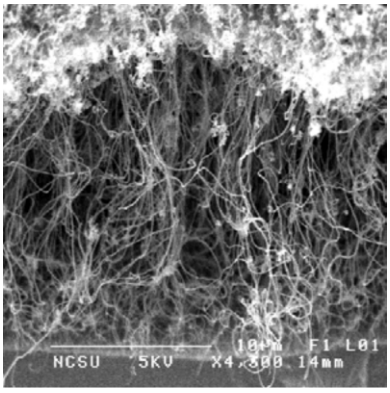

Fig. 1. An SEM image of the CNT film grown for 15 min.

temperature ramp was initiated until the substrate temperature reached 600 °C, ammonia and acetylene precursors were fed into the chamber at a flow rate of 70 sccm and 18 sccm, respectively, and the plasma was ignited. Other growth parameters were: substrate temperature of 900 °C, pressure of 20 Torr, and plasma power of 600 W. The samples were characterized by SEM (JOEL 6400F) and Raman spectroscopy. TEM was used to observe the internal structure of the carbon nanotubes. The TEM specimens were prepared from CNT, which were scraped from the as-grown film, and sonically dispersed in alcohol. A carbon TEM microgrid was then immersed into the alcohol, and the microgrid was dried in air. The adsorbed CNT were then imaged in the TEM.

3. Results

Fig. 1 shows an SEM image of a CNT film grown for 15 min. The sample is characterized as a carbon nanotube 'forest' with a thickness of ~20 μm. The multiwalled CNT, with an average diameter of ~100 nm, are mostly vertical but significant curvature and deviations from vertical are observed. Amorphous carbon is evident on the film surface.

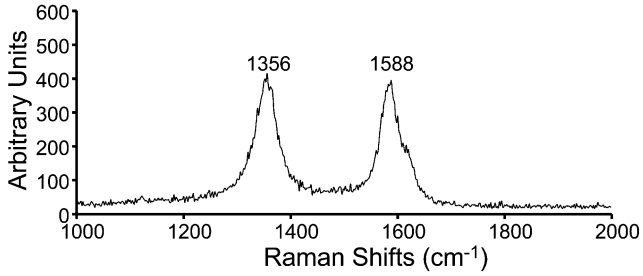

Fig. 2. Raman spectrum of the 15 min carbon nanotube sample. The spectrum was acquired with 514.5 nm excitation.

A macro-Raman spectrum of the 15 min CNT sample is shown in Fig. 2. The spectrum shows peaks of 1588 cm^{-1} (G mode) and 1356 cm^{-1} (D mode), which have been reported for carbon nanotubes [16]. The G mode represents in-plane vibration of C atoms in the graphite sheet, while the D mode is ascribed to disordered sp^2 carbon and explained as defects in the curved graphite sheet and tube ends [17] or the curved parts of carbon nanotubes [16].

To study the growth of CNT, we prepared another sample with a growth time of 30 min. We found that the growth time strongly affects the structure and morphology of the film. The Raman spectrum of the sample was similar to that of the 15 min growth. An SEM image of the film with a growth time of 30 min is shown in Fig. 3a. The film thickness is approximately 50 μm, and two separate layers are apparent in the film (see arrows). Fig. 3b shows an image of the top layer of the film, where a 5–7 μm thick CNT mat is mixed with amorphous carbon. Fig. 3c shows the bottom layer of the same film. Here, the carbon nanotube 'forest' is similar to the 15 min sample but with a thickness of approximately 30 μm.

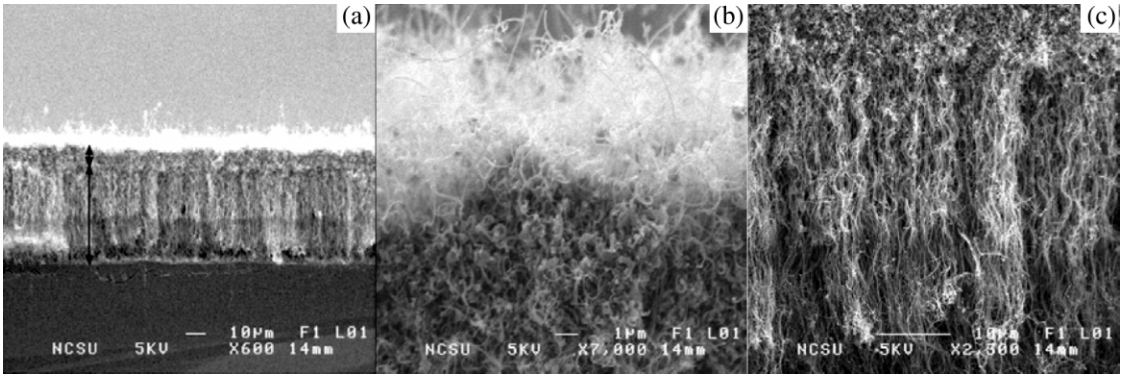

Fig. 3. SEM images of (a) a CNT film grown for 30 min, where the film exhibits two identifiable layers (see arrows); (b) the top layer of the film, where the surface is covered by a carbon nanotube mat and amorphous carbon, (c) and the bottom layer of the film, where it appears that carbon nanotube forest similar to the 15 min sample.

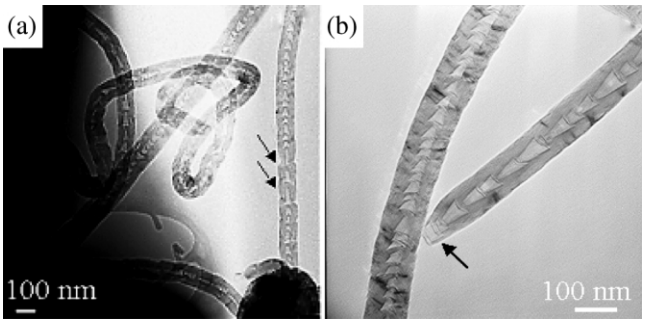

Fig. 4. Low magnification TEM images of (a) CNT with bamboo structure. An iron particle with a hemispherical shape is shown in the lower right corner of the figure. Arrows show several elongated and relatively cylindrical compartments. (b) A tube with a tip free of a catalyst particle (see arrow).

The amorphous carbon is apparently a byproduct of the MPCVD process, and it appears that the deposition may have occurred throughout the growth. Eventually, this layer is mixed with a CNT mat. It is noted that the growth rate of the CNT 'forest' (the bottom layer for 30-min sample) is reduced from that of the 15-min growth. The 30-min sample showed a growth rate of $\sim$1 μm/min, while the 15-min sample with a thickness of 20 μm, exhibited a growth rate of $\sim$1.33 μm/min. The reduced growth rate may be due to a reduction of the supply of carbon species reaching the catalyst layer as the amorphous carbon and CNT mat forms on the film surface.

TEM of the CNT samples show bamboo structure with periodic empty compartments in the tubes. Fig. 4a is a low magnification TEM image, and an iron particle can be observed with a hemispherical shape. It is also noticeable that the shape and dimension of each compartment changes along the tubes. Although most compartments have a cone-like shape, several elongated and relatively cylindrical compartments are observed (see arrows). Fig. 4b shows a tube with a tip free of a

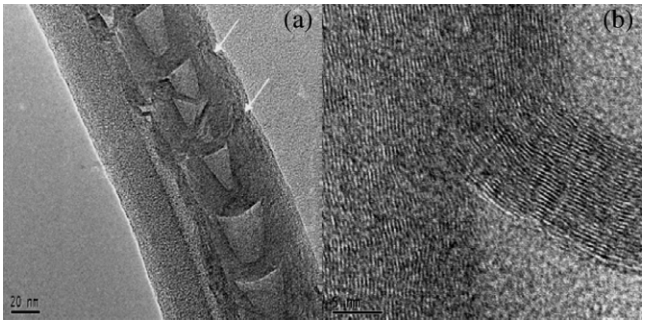

Fig. 5. (a) A high magnification TEM image of a single CNT. The arrows show a wave-like deposition along the tube walls, and (b) a high resolution TEM image of the joint of the inter layers and tube walls.

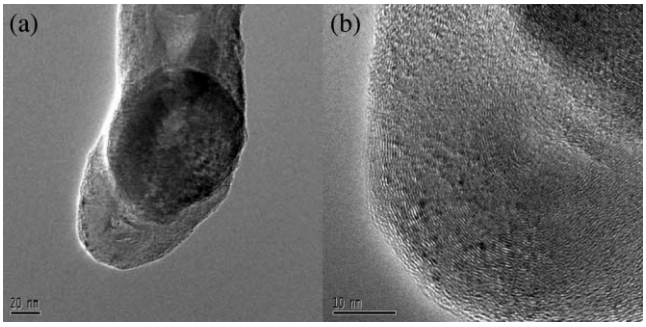

Fig. 6. (a) A TEM image of a tube tip with an encapsulated catalyst. A cone-like compartment terminates at the upper end of the catalyst particle sphere, and (b) a higher resolution TEM image of the tip.

catalyst particle. The tip has a closed structure, which is apparently capped with graphitic layers. The presence of CNT tips free of catalyst particles indicates that the growth of our carbon nanotube film favors the base growth model.

Fig. 5a displays a high magnification TEM image of a single carbon nanotube. The arrows show a wave-like deposition along the tube walls, which may be due to the deposition of amorphous carbon along the tube walls during growth. Fig. 5b is a high resolution TEM image of the joint of the inter layers and tube walls. The inter-graphitic layers between two compartments have $\sim$30 graphitic sheets with a thickness of $\sim$12 nm.

A catalyst encapsulated tip was also observed in the same sample. Fig. 6a displays images of tip with an encapsulated catalyst particle. The origin of these catalyst encapsulated tips is not established, but it is likely that the catalyst will affect the structure of the compartments near the particle.

To determine the relative abundance of catalyst particles at the surfaces we employed Auger electron spectroscopy (AES) for chemical analysis. Fig. 7 shows

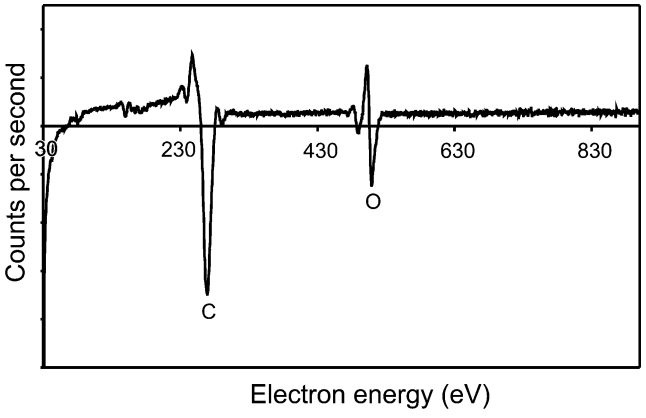

Fig. 7. AES Chemical analysis of the surface of the 15 min CNT film. The spectrum displays features due to C and O and no evidence of the Fe related peak at 703 eV.

the AES of the 15 min CNT film surface. A similar spectrum was observed for the 30 min film. The spectra are dominated by a strong carbon peak with a weaker oxygen peak apparently due to adsorbed species. There was no evidence of the Fe peak that occurs near 703 eV, which suggests a very small amount of iron at the CNT tips. A similar sample was examined after H-plasma etching to remove the disordered carbon layer at the surface, and again there was no evidence of Fe in the AES.

4. Discussion

The TEM results show that there are tube tips that are free of the catalyst, and the curvature of the inter layers between the compartments are directed toward the carbon nanotube tips. Although Fig. 6a exhibits a tube tip with an encapsulated catalyst particle, Auger analysis of the CNT surface shows that essentially no iron was detected, which indicates that most tube tips are free of the catalyst particles. This leads us to conclude that the base growth mode predominates in our CNT growth. This conclusion is consistent with other studies of MPCVD growth of CNT [8].

In addition, Bonard et al. [18] used electron field emission measurements to monitor the growth of carbon nanotubes by chemical vapor deposition. It was shown that electron field emission from a growing tube presents a single, homogeneous spot, which was interpreted to indicate that the carbon nanotube has a closed cap, and it is the first part of the nanotube to be formed. They also observed that the catalyst was attached to the substrate. Although the partial pressure of hydrocarbons in their chamber was four orders of magnitude lower than conventional CVD due to the requirements of field emission, this experiment provides another perspective of the CNT growth mode.

The 30 min growth sample showed a decrease in the growth rate of the aligned CNT forest. At the same time, excess carbon species was observed to form amorphous carbon deposits around the CNT and at the top surface of the film. The amorphous carbon deposits were not observed at the roots of the nanotube forest. A possible explanation for the reduction in growth rates is that as the layer of amorphous carbon and carbon nanotube mat becomes thicker, and these structures inhibit the diffusion of carbon species reaching the catalysts attached to the substrate.

The mechanism for the formation of the bamboo mode structures of the carbon nanotubes is also intriguing. Among the many proposals used to explain this phenomenon, it has been suggested that the bamboo structures may be due to the catalyst particle shape, carbon diffusion in the catalyst, or the slow movement of the catalyst compared to the growth rate of carbon nanotubes [7,11–13]. The moving catalyst model is not appropriate, since it cannot explain the bamboo structure of the carbon nanotubes with the tips free of catalyst particles. While the catalyst shape may contribute to the nanotube formation, we suggest that the difference between the carbon surface and bulk diffusion in the catalyst causes the periodic compartment structures [11]. In this model the carbon species would react with, diffuse into, and precipitate out of the catalyst to form the carbon nanotubes. The walls of the carbon nanotubes are formed from the side surface of the catalyst mainly via carbon surface diffusion while the inter layers form from the catalyst top surface via bulk diffusion. Since there are different diffusion rates for carbon to move along the catalyst surface and through the bulk of the catalyst, the growth rate of the walls and inter layers may be different, which leads to the formation of periodic compartments.

It was observed in our samples that most compartments have cone-like structures, but several long relatively cylindrical structures are also found in the same tubes. This result suggests that the catalyst shape alone cannot explain the presence of different compartment dimensions in a single tube. It is likely that the different compartment formation is related to changes in the CNT growth rate, which could be influenced by the supply of the carbon containing species and possibly the presence of contaminants on the surface.

5. Summary

In summary, aligned carbon nanotube films were prepared by MPCVD, and the samples were characterized with SEM, TEM, and Raman spectroscopy. The results show multiwalled CNT with bamboo mode structures. Auger analysis of the CNT film shows no detectable Fe at the film surface, suggesting that the base growth model predominates for this MPCVD growth. The sample grown for 30 min exhibits a CNT ‘forest’ with a surface layer composed of a CNT mat and amorphous carbon. The growth rate decreases with time, and we suggest that the surface layer limits the supply of carbon containing species to the catalyst. The different shapes of the compartments in the CNT indicate that the interplay between the catalyst and the precursor gases will affect the carbon surface and bulk diffusion in the catalyst.

Acknowledgments

This research is supported by the ONR-MURI on Thermionic Energy Conversion and the DOE-center of Excellence for Synthesis and Processing of Carbon-Based Nanostructures.

References

[1] H. Dai, Surf. Sci. 500 (2002) 218.
[2] J. Kwo, M. Yokoyama, C. Lee, F. Chuang, I. Lin, J. Vac. Sci. Technol. B 19 (3) (2001) 1023.

[3] K. Xiao, Y. Liu, P. Hu, G. Yu, X. Wang, D. Zhu, Appl. Phys. Lett. 83 (2003) 150.
[4] S. Ghosh, A.K. Sood, N. Kumar, Science 299 (2003) 1042.
[5] A.M. Fennimore, T.D. Yuzvinsky, W. Han, M.S. Fuhrer, J. Cumings, A. Zettl, Nature 424 (2003) 408.
[6] J-C. Charlier, A.D. Vita, X. Blase, R. Car, Science 275 (5300) (1997) 647.
[7] L. Yuan, T. Li, K. Saito, Carbon 41 (1889) 2003.
[8] C. Bower, O. Zhou, W. Zhu, D.J. Werder, S. Jin, Appl. Phys. Lett. 77 (2000) 2767.
[9] D. Li, L. Dai, S. Huang, A.W.H. Mau, Z.L. Wang, Chem. Phys. Lett. 316 (2000) 349.
[10] R.T.K. Baker, Carbon 27 (1989) 315.
[11] C.J. Lee, J. Park, Appl. Phys. Lett. 77 (2000) 3397.
[12] G.Y. Zhang, X.C. Ma, D.Y. Zhong, E.G. Wang, J. Appl. Phys. 91 (2002) 9324.
[13] V.V. Kovalevski, A.N. Safronov, Carbon 36 (1998) 963.
[14] C. Bower, O. Zhou, W. Zhu, D.J. Werder, S. Jin, Appl. Phys. Lett 77 (2000) 830.
[15] F.A.M. Kock, J.M. Garguilo, R.J. Nemanich, Diam. Relat. Mater. 10 (2001) 1714.
[16] Y.S. Jung, D.Y. Jeon, Appl. Surf. Sci. 8154 (2002) 1.
[17] G. Maurin, Ch. Bousquet, F. Henn, P. Bernier, R. Almairac, B. Simon, Solid State Ionics 136–137 (2000) 1295.
[18] J-M. Bonard, M. Croci, C. Klinke, F. Conus, I. Arfaoui, T. Stockli, et al., Phys. Rev. B 67 (2003) 085412.